ACS Sustainable Chemistry & Engineering

pubs.acs.org/journal/ascecg

Research Article

Transfer of Poly(methyl methacrylate) Nanoparticles from Parents to Offspring and the Protection Mechanism in Two Marine Invertebrates

Yong Jie Yip, Gayathiri D/O Sivananthan, Serina Siew Chen Lee, Mei Lin Neo, Serena Lay-Ming Teo,* and Suresh Valiyaveettil*

Cite This: *ACS Sustainable Chem. Eng.* 2022, 10, 37−49

Read Online

ACCESS | Metrics & More | Article Recommendations | Supporting Information

ABSTRACT: Ingested nano- and microplastic particles are observed to cause significant health impacts in several animal models. In this study, we investigate the nanoplastic particle transfer from exposed adults to offspring using the marine calcareous tubeworm *Spirobranchus bakau* and the acorn barnacle *Amphibalanus amphitrite* as model organisms. Adult tubeworms and barnacles were exposed to blue fluorescent poly(methyl methacrylate) (PMMA) nanoparticles at 10 mg/L concentration for 12 and 25 days, respectively, under controlled environmental conditions. PMMA nanoparticles used in the exposure experiments had a hydrodynamic size of 167.7 nm when dispersed in ultrapure water (DLS), a dry size of 106.4 nm (SEM), and a zeta potential of −28.4 mV. PMMA particles were found on the membrane of sub-mantle tissues in adult barnacles but not in the oocytes or developing embryos of barnacles. On the other hand, PMMA nanoparticles were observed inside the eggs of tubeworms. After fertilization, these PMMA nanoparticles were gradually released from the developing embryos via exocytosis, and no PMMA particles were observed inside the trochophores 24 h post-fertilization. In addition, the PMMA nanoparticles present during early developmental stages of the tubeworm eggs did not affect trochophore development or subsequent settlement. Based on the two model species tested, the results suggest that the protective mechanisms preventing transfer of nanoparticles of common plastics from parents to offspring could differ among animal species and that the choice of the animal model and the size of polymer nanoparticles selected can significantly impact the outcome of the study.

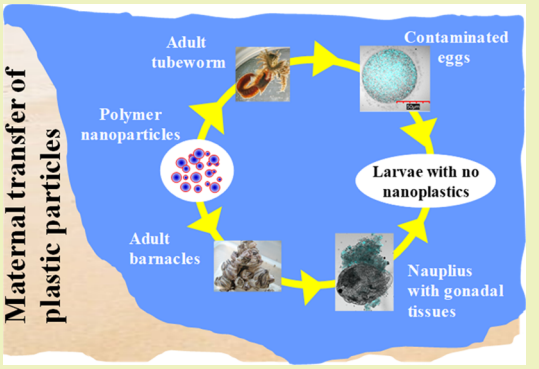

KEYWORDS: *microplastics, nanoplastics, maternal transfer, toxicity, marine invertebrates*

INTRODUCTION

Recent studies highlight the accumulation and release of used plastic articles and small particles in the marine environment at high concentrations.[1−6] Smaller particles are estimated from current plastic pollution levels to occur in the pg/L and μg/L ranges;[7] however, significant concentration variation can be expected between different biomes. Such micro- and nanoparticles of common plastics pose serious health and environmental concerns to living organisms and the overall ecosystem health, respectively.[8,9] Microplastics have been loosely defined as polymer fragments smaller than 5 mm, while nanoplastics are defined as polymer particles smaller than 1 μm.[10] While there is no consensual definition for their size threshold, nanoplastics are defined as polymer particles smaller than 1000 nm in the present study. Although multiple methods have been proposed for the isolation and characterization of nanoplastics from the environment, the complex matrix present in environmental samples has largely prevented nanoplastic isolation and quantification.[11] Owing to the small size, large surface area, and multiple surface functional groups, the potential impacts of nanoplastics on organisms and the environment have been the subject of several studies.[12−14]

The toxicity and retention time of micro- and nanoplastic particles in living organisms have been shown to increase with a decrease in particle size.[15−18] Ingested micro- and nanoplastics have been shown to translocate by absorption through the lumen of the digestive tract of various animal models in both invertebrates[14,19] and vertebrates.[13,20,21] While translocation mechanisms of micro- and nanoplastics are not explained in detail for most studies, there is evidence to show that plastic nanoparticles are small enough to translocate from

Received: March 19, 2021
Revised: December 9, 2021
Published: December 27, 2021

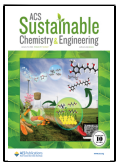

https://doi.org/10.1021/acssuschemeng.1c01818
ACS Sustainable Chem. Eng. 2022, 10, 37−49

the digestive tract to other tissues[22] and reach the internal organs such as the liver,[20,21] brain,[23] hemolymph,[24] and gonads.[19] In earlier studies, embryos collected from exposed *Danio rerio* females showed the presence of polystyrene (PS) nanoparticles with an average diameter of 42 nm,[13] while transfer of larger PS nanoparticles (average size—100 nm) to offspring via translocation from the gonadal tissues to eggs was seen in *Caenorhabditis elegans*.[19] Small amounts of maternally transferred virgin PS nanoparticles induced bradycardia and reduced glutathione reductase and thiol levels in *D. rerio* larvae.[13] Similarly, PS nanoparticles caused transgenerational toxicity in *C. elegans*.[19] The detrimental effects of polymer particles on reproduction will eventually lead to a reduction in the overall health of populations of vulnerable species living in a contaminated ecosystem.

Here, we examined the potential for the transfer of fluorescent poly(methyl methacrylate) (PMMA) nanoparticles from parents to the offspring of two common mangrove inhabitants, the calcareous tubeworm, *Spirobranchus bakau* (*S. bakau*), which was recently described[25] [as *S. kraussii* (Baird, 1864) in Chan et al.,[26,27] phylum: Annelida, family: Serpulidae], and the acorn barnacle, *Amphibalanus amphitrite* (*A. amphitrite, phylum: Arthropoda, subphylum: Crustacea*).

Coastal ecosystems such as mangroves are particularly vulnerable to plastic pollution due to their proximity to various sources of land-based plastic debris. Jambeck et al. reflected that the reported amount of floating plastic debris in the open ocean is 1−3 orders of magnitude lower than their estimates of the quantity of land-derived plastics entering the ocean,[28] and this difference may be accounted for by plastics retained in coastal habitats such as mangroves.[29] Additionally, mangrove forests are structurally more complex than open shores such as sandy beaches and therefore are inherently more efficient in trapping plastic debris and facilitating their deposition and fragmentation,[29,30] leading to mangroves becoming sinks of microplastics and ultimately nanoplastics. However, there is presently a lack of studies on the impacts of nanoplastics and the potential for them to be maternally transferred in marine invertebrates inhabiting coastal environments.[31]

Transitioning to a sessile mode of life from a planktonic larval stage, tubeworms and barnacles become permanently attached to substrates. Their sessility likely subjects them to the risk of chronic exposure to plastic particles in their ambient environment, albeit at lower concentrations than in mangrove sediments.[32] Hence, as sessile fauna of mangrove habitats, *S. bakau* and *A. amphitrite* make ecologically relevant model organisms for this study to address the knowledge gap concerning the impacts of nanoplastics on coastal organisms and the potential for maternal transfer of plastic particles to the next generation. The planktonic larvae of both animals also form part of the zooplankton consortia, which are an important food source for transferring energy to higher trophic levels. Nanoplastic contamination may have implications for transferring nanoplastics up the trophic web. The transparency of their gametes and larvae also makes them favorable for microscopic visualization of fluorescent PMMA nanoparticles.

The two selected model organisms employ different reproduction methods. For *A. amphitrite*, fertilization and development of the embryo to the first naupliar instar occur inside the mantle cavity, whereas the calcareous tubeworm *S. bakau* is a dioecious broadcast spawning invertebrate. These differences between the reproductive modes and life cycles of the two species provided additional reasons to use them as model organisms to investigate the influence of the reproductive strategy of marine invertebrates on the potential maternal transfer of nanoplastics.

PMMA was selected as the nanoplastic analogue. We reported that PMMA nanoparticle exposure is nontoxic at up to 25 mg/L,[14,33] and optically transparent monodispersed PMMA nanoparticles can be prepared via precipitation in water.[34] The hydrophobic blue fluorophore, perylene, is compatible with PMMA encapsulation and showed no leaching in water or seawater. *S. bakau* is found in coastal mangrove biomes where plastic pollution is high,[35] hence they can be expected to tolerate moderate nanoplastic exposure. Exposure of adult *A. amphitrite* to PS microbeads at up to 1000 beads/mL was reported to not affect survival and larval development,[36] indicating that *A. amphitrite* has high tolerance for polymer particle exposure, making them suitable for the present study. Both model organisms are expected to tolerate exposure to PMMA nanoparticles at moderate to high concentrations. We reported earlier that *A. amphitrite* nauplii ingest and retain PMMA nanoparticles in their body but develop into the juvenile stage without observable deformations or toxicity.[14]

The effects of PMMA nanoparticle exposure have not been reported widely as most nanoplastic literature has focused extensively on PS as a model nanoplastic.[31] In fact, PMMA nanoparticles did not have adverse interactions with the microalgae *Tetraselmis suecica* and *Chaetoceros muelleri*[14] used as the microalgal feed for sustaining *A. amphitrite* adults in this study. The growth of a few marine microalgae species, *Tetraselmis chuii*, *Nannochloropsis gaditana*, *Isochrysis galbana*, and *Thalassiosira weissflogii*, was adversely affected by 39 nm PMMA nanoparticles only at high concentrations between 19 and 214 mg/L, although the rotifer *Brachionus plicatilis* was found to be more sensitive to PMMA nanoparticle exposure with an $LC_{50,48h}$ of 13.3 mg/L.[37] However, exposure of *Sparus aurata* to 45 nm PMMA nanoparticles was reported to increase mRNA transcription of genes related to lipid metabolism and activate antioxidant defense after 24 h of exposure.[38] This suggests that PMMA nanoparticle exposure is unlikely to be toxic at low to moderate concentrations, but toxic responses may vary significantly between different organisms.

We hypothesized that ingested nanoplastics are small enough to translocate into the gonads of the two model animals, as observed in *C. elegans*,[19,39] and potentially transfer to the gametes and offspring of the exposed animals. Maternal transfer of nanoplastics can have significant ramifications on entire ecological systems as any detrimental effects on reproduction caused by nanoplastics could negatively affect an entire animal population. Adult individuals of *A. amphitrite* and *S. bakau* were hence exposed to PMMA nanoparticles to investigate the possible inheritance of PMMA nanoparticles by the offspring.

METHODS AND MATERIALS

Preparation of Fluorescent Tagged PMMA Nanoparticles. Polymer nanoparticle dispersions were prepared via precipitation from an organic solution to yield spherical particles with good monodispersity.[14,34] A blue fluorescent perylene dye was encapsulated in the PMMA nanoparticles to minimize interference from the intracellular autofluorescence in the range of 540 and 560 nm.[40,41] The chosen perylene fluorophore emits intense blue fluorescence upon excitation and is highly hydrophobic, making it compatible for

https://doi.org/10.1021/acssuschemeng.1c01818
ACS Sustainable Chem. Eng. 2022, 10, 37−49

the polymer precipitation method used for particle synthesis, prevents leaching from the particle, and allows for easy for optical detection.[34]

PMMA (15 kDa, 400 mg), perylene (4 mg, 1 wt %), and sodium dodecylsulfate (8 mg, 2 wt %) were dissolved in acetone (100 mL). A small volume of the solution (5 mL) was quickly added to water (50 mL) and stirred continuously over 18 h for acetone to evaporate. The size and zeta potential of the prepared PMMA nanoparticles were obtained from dynamic light scattering (DLS) measurements using a Malvern Zeta Sizer instrument. The nanoparticle morphology was characterized using a JEOL JSM-6701F field emission scanning electron microscope (SEM). Briefly, the nanoparticle dispersion was drop-cast on a glass coverslip from ultrapure water and sputter-coated with platinum before imaging in SEM. The absorbance spectrum of the PMMA nanoparticles was recorded on a UV-1800 Shimadzu UV−Visible spectrophotometer, while the emission spectrum was obtained from an Agilent Cary Eclipse Fluorimeter. Optical characterization of the polymer nanoparticles was conducted in ultrapure water.

Aggregation of Nanoparticles in Seawater. To understand the effects of seawater on the aggregation of PMMA nanoparticles, the prepared nanoparticles (0.5 mL, a 10 mg/L final PMMA nanoparticle concentration) were added to 0.22 μm filtered seawater (20 mL) adjusted to 27 practical salinity units (PSU) and left to stand for 24 h before the size of the PMMA nanoparticle aggregates was measured using DLS. The DLS measurement was performed in triplicate, and the average value was reported. The aggregation of PMMA nanoparticles in seawater was assessed at the salinity both model organisms were exposed at to determine the PMMA nanoparticle aggregate size the animal models were exposed to. The PMMA nanoparticle aggregate sizes were assessed at 24 h to allow for an adequate time for particle aggregation to stabilize. As the exposed animals were exposed to fresh doses of PMMA nanoparticles every alternate day, the PMMA aggregates formed at 24 h would be representative of the average aggregate sizes ingested by the exposed animals.

A seawater salinity of 27 PSU was selected to balance both the survival needs of the model organisms used in the study and yet not cause extensive aggregation of the PMMA nanoparticles that they form large flocs that settle out of the water column. Both *S. bakau* and *A. amphitrite* were found to thrive at salinity ranges encompassing 27 PSU[25,42] and were hence maintained at 27 PSU in this study. They were collected from mangroves along the northwest coast of Singapore, often with brackish water due to rainwater runoff and riverine inputs, predominantly from two major rivers in Johor (Sungei Pulai and Sungei Johor).[43]

Leaching of Perylene from PMMA Nanoparticles. The potential for the perylene fluorophore to leach from the PMMA nanoparticle was tested via a reported method.[44] Undiluted PMMA nanoparticle dispersion in ultrapure water (10 mL, 400 mg/L) was sealed inside a SnakeSkin dialysis membrane (a 3.5 kDa molecular weight cutoff), and the whole tube was immersed in ultrapure water (200 mL). A control sample was implemented in an identical setup with only ultrapure water (10 mL) placed in the dialysis membrane tube instead of the PMMA nanoparticle dispersion. Fluorescence of the dialysate from both the PMMA nanoparticle leaching experiment and control experiment was checked after 72 h using an Agilent Cary Eclipse Fluorimeter at 405 nm excitation.

Nanoparticle Exposure Conditions. Two nontoxic exposure concentrations were tested during preliminary trials—5 and 10 mg/L. Eggs from tubeworm adults exposed to PMMA nanoparticles at 10 mg/L were found to exhibit greater fluorescence under confocal microscopy. The PMMA nanoparticle exposure concentration had to be high enough for maternally transferred PMMA nanoparticles to be detectable and yet low enough to not cause any toxicity or interfere with reproduction in the exposed animals. Appropriate numbers of barnacles (25) or tubeworms (8−11) kept inside a glass beaker were exposed to PMMA nanoparticles with a hydrodynamic radius of 167 nm at a concentration of 10 mg/L (effectively 1.32×10^{13} particles per liter) in 27 PSU seawater to investigate the intake and maternal transfer to their offspring.

Exposed animals were then cleaned externally and depurated for 24 h in clean seawater before they were spawned, or their gametes were sampled. A depuration period of 24 h was selected as the process required the animals to be maintained sans feed. Depuration could be neither be too long such that starvation induces mortality nor too short for the egestion of unassimilated PMMA nanoparticles. A 24 h period was determined to be an appropriate length of time for the depuration process.

Field Collection and Maintenance of Animals. All barnacles and tubeworms used in this study were collected from mangroves along the northwest coast of Singapore and maintained at the indoor aquaria facility of St John's Island National Marine Laboratory, Singapore, prior to experimental use.

Exposure of *A. amphitrite* Adults to PMMA Nanoparticles. Prior to start of the exposure experiment, the freshly collected barnacles were cleaned of mud and fouling then spawned to release any larvae brooded in the adults. Clusters of 20−25 adults of *A. amphitrite* were suspended in aged seawater (27 PSU, 500 mL) in glass beakers. Each treatment—exposure to PMMA nanoparticles and control—was conducted with three replicates. A mixed microalgae diet of 1:1 *T. suecica* and *C. muelleri* (50,000 cells/mL) and freshly hatched brine shrimps (Bio-Marine; 20 nauplii/mL) were added as feed. Full water change and feed replenishment were carried out every alternate day for all treatment samples. PMMA nanoparticles were dosed into the PMMA exposure treatment beakers only (12.5 mL, a 10 mg/L final concentration), and control samples did not have any polymer particles. All test samples were kept inside a growth chamber at 28 °C under a 12 h light/12 h dark cycle with gentle aeration to keep feed and PMMA nanoparticles in suspension. Initially, barnacles were spawned after 7, 14, and 21 days of exposure; barnacles were scrubbed clean, rinsed with fresh water, and dried overnight to induce spawning. However, PMMA nanoparticles were not detected in any of the nauplii collected from exposed barnacle adults did not show appreciable fluorescence under confocal microscopy. The experiment was then terminated after 25 days. The barnacles were carefully cleaned to remove any particles on the shells and transferred to clean seawater to depurate for 24 h without feed or PMMA nanoparticles. A depuration period of 24 h was selected to allow for the egestion of unassimilated PMMA nanoparticles. Egg lamellae containing developing embryos and/or tissues containing oocytes were removed from both barnacles exposed to PMMA particles and control treatment samples and imaged via confocal microscopy to ascertain the presence and distribution of PMMA nanoparticles.

The relatively large number of exposed barnacles per treatment (25) was necessary to produce adequate numbers of nauplii because each barnacle releases relatively few nauplii at each spawning.

Exposure of *S. bakau* Adults to PMMA Nanoparticles. Prior to start of the exposure experiment, external surfaces of tubeworms were cleaned of mud and fouling. Each treatment—exposure to PMMA nanoparticles and the control—was conducted with six replicates. A total of 8−11 worms were maintained per replicate in a clear glass dish with aged seawater (150 mL) at a salinity of 27 PSU. All tubeworms were acclimatized to the experimental setup for 10 days prior to the start of the experiment, during which microalgae, *Tisochrysis lutea* (*T. lutea*), were supplied as feed (300,000 cells/mL). Full water change and feed replenishment were carried out three times per week. An acclimatization period was deemed to be necessary because mortalities were usually observed among the tubeworms, regardless of their treatment group, within the initial few days of being placed into the experimental setup during preliminary trials. During the experimental period, all tubeworms continued to be fed *T. lutea* (300,000 cells/mL) three times per week after total water change. The tubeworms from only the PMMA exposure treatment beakers were dosed with PMMA nanoparticles (3.75 mL, a 10 mg/L final concentration) along with algal feed. From preliminary trials where tubeworms were subjected to nanoplastic exposure for 10, 11, 12, 14, and 24 days, we concluded via confocal imaging of the eggs collected from exposed adults that an exposure duration of 12 days was sufficient for allowing maternal transfer of PMMA nanoparticles to their eggs. All sample dishes were kept inside a growth chamber at

https://doi.org/10.1021/acssuschemeng.1c01818
ACS Sustainable Chem. Eng. 2022, 10, 37−49

28 °C with gentle aeration under a 12 h light/12 h dark cycle. After exposure, tubeworms were carefully cleaned with a soft brush to remove any particles on their tubes and transferred to clean seawater to depurate for 24 h in the absence of feed and PMMA nanoparticles. The tubeworms were gently removed from the water after depuration and used for gamete collection.

A total of 8 to 11 tubeworms were maintained per replicate to provide enough gametes for imaging and downstream trochophore culture experiments, while maintaining an optimum ratio of individuals to the volume of seawater per replicate to minimize stress to the animals resulting from competition for feed, buildup of waste products, and deteriorating water quality. Moreover, it is challenging to determine the sexes of gonochoristic calcareous tubeworms such as *S. bakau* without cracking open their tubes to expose their abdomen, the color of which is indicative of their sex. Therefore, there was a need to include an adequate number of animals per treatment to buffer against the inherent uncertainty in the number of male and female tubeworms to eventually provide a sufficient number of gametes for the study.

***S. bakau* Fertilization and Embryonic Development.** *Gamete Collection.* Gamete release was artificially induced in individual tubeworms by cracking open their tubes.[45] Eggs were pooled from a total of 11−16 females across the 6 replicates for each treatment and concentrated in aged seawater (10 mL, 27 PSU), resulting in a suspension of approximately 300 eggs/mL. The sperm was similarly pooled for each treatment and stored in a fridge for no longer than 30 min until use. A sub-sample (5) of unfertilized eggs collected from adults exposed to the PMMA nanoparticles and control tubeworms was imaged under a confocal microscope, while the remaining eggs were fertilized. The eggs collected from tubeworms exposed to PMMA particles showed luminescent particles inside the eggs, indicating that the maternal transfer has occurred in tubeworms.

Fertilization and Development. The sperm collected from tubeworms exposed to PMMA nanoparticles and control tubeworms was added dropwise into egg suspensions from their respective treatments until the solution just turned cloudy. The egg−sperm suspension was left to stand for 5 min before diluting to a final volume of 300 mL. A minimum of three developing eggs was sampled randomly from each treatment every 2 h for imaging until trochophore larvae hatched 17 h post fertilization (hpf). Although the number of developing embryos sampled in each time point was small, each sample of three eggs from different time points collectively provided information on what was happening inside the developing embryos during the entire developmental stage. The sampling size for each time point also had to be limited to ensure that a sufficient number of eggs, accounting for natural mortality, were maintained for subsequent sampling time points.

The blastulae were immobilized using copper sulfate solution (0.1%) instead of fixing with glutaraldehyde to prevent interference from autofluorescence caused by Schiff's base structure formation.[46,47] Confocal microscope settings were determined using unfertilized eggs from the PMMA nanoparticle-exposed individuals which showed fluorescence from the nanoparticles.

***S. bakau* Trochophore Culture.** The trochophores obtained from fertilization of eggs collected from adult tubeworms exposed to PMMA nanoparticles and control parents were cultured in six-well cell culture plates for 10 days, with 10 replicate wells set up for each treatment. A total of 30 healthy, swimming trochophores were maintained in each replicate well containing clean aged seawater (10 mL, 27 PSU) and fed a mixed microalgal diet of 1:1 *T. lutea* and *Nannochloropsis oceanica* (50,000 cells/mL). All well plates were maintained in a growth chamber at 28 °C under a 12 h light/12 h dark cycle. Once every 2 days, the number of normal and abnormal trochophore developments was scored on a Bogorov tray. Abnormalities included abnormal size and/or shape and mortalities. Successful settlement (indicated by the presence of at least a primary, transparent tube) of the trochophores in the well plates was also recorded. After scoring, the larvae were transferred back into the wells of the six-well plates pre-filled with fresh filtered seawater and microalgal feed. Proportion of normal trochophores is expressed as the proportion of surviving larvae (as enumerated on the previous scoring day) with normal development. Larval settlement was observed in both treatments from the sixth day of culture onward. Proportion of settled larvae is expressed as the proportion of surviving larvae (as enumerated on the previous scoring day, i.e., days 4, 6, and 8) that have settled. The statistical significance of differences in the proportion of normal development and settlement between trochophores obtained from tubeworms exposed and unexposed (control) to PMMA nanoparticles was determined via a one-tailed *t*-test.

Fluorophore Extraction from Developing *S. bakau* Eggs. In order to complement the confocal microscopy images obtained from trochophores, another independent extraction experiment was designed to detect the fluorophore. The extraction experiment was run in 6 replicates, with a total of 27−30 worms maintained per replicate in 500 mL of filtered aged seawater at a salinity of 27 ± 1 PSU. Exposure of *S. bakau* tubeworms to PMMA nanoparticles, gamete collection, and fertilization were carried out according to the protocols described above. Unfertilized eggs (0 hpf) and trochophores (24 hpf) were sampled for analysis. Each sample was washed with clean filtered seawater using a 35 μm sieve to remove any polymer nanoparticles in the water column. All washed egg and trochophore samples from PMMA nanoparticle-exposed and control groups were resuspended separately in filtered seawater (20 mL, 27 PSU) and digested by the addition of hydrogen peroxide (5 mL, 6% final concentration) at 60 °C for 20 h. The digested aqueous sample was extracted with dichloromethane (DCM, 20 mL), and the organic fraction was examined using fluorescence spectroscopy by using an excitation wavelength of 405 nm to determine the presence of perylene.

Imaging Methods. All samples and materials collected from tubeworms and barnacles were imaged immediately after release or dissection via confocal microscopy to avoid contamination or degradation. Laser power and fluorescence signal amplification were adjusted to prevent detector saturation. The offset value was adjusted to mitigate background noise. All samples were imaged using the same settings to yield comparable micrographs. Since the samples were not fixed with glutaraldehyde, no autofluorescence was detected. All samples were imaged using an Olympus FV3000 or Zeiss LSM 900 confocal microscope under identical settings. At least five unique *S. bakau* eggs from each treatment were imaged under DAPI and the transmitted light mode. An excitation wavelength of 405 nm was used, and the emission spectrum was collected between 430 and 470 nm. Fluorescence intensities from confocal fluorographs were quantitated using ImageJ analysis. Statistical significance of differences between average fluorescence intensities of the confocal fluorographs from PMMA nanoparticle-exposed and control groups was determined via one-tailed *t*-tests.

RESULTS AND DISCUSSION

Preparation of Fluorescent Tagged PMMA Nanoparticles. PMMA nanoparticles encapsulated with the luminescent perylene dye were prepared using a previously published procedure.[14,34] Full characterization data are given in the Supporting Information, Figure S1. The size measurements of the PMMA nanoparticle dispersion in ultrapure water was performed using DLS, which gave an average size of 167 nm with a dispersity index of 0.1. The zeta potential of the PMMA nanoparticles was determined to be −28.4 mV. The average diameter of the spherical dry particles obtained from SEM was 106.4 nm, which is expectedly smaller than the hydrated value obtained from DLS measurements. The luminescent PMMA nanoparticles showed strong absorbance at 412 nm and emission at 441 nm (Figure S1B, typical of perylene) in water with little or no significant photobleaching within a few months. Hence, perylene is suitable for optical imaging using a confocal microscope with a 405 nm laser source for excitation.

https://doi.org/10.1021/acssuschemeng.1c01818
ACS Sustainable Chem. Eng. 2022, 10, 37−49

From our earlier investigations, it was established that the fluorophore aggregation was minimum inside the polymer particle and no aggregation-induced fluorescence quenching was observed.[34] The emission intensity of the polymer nanoparticle dispersion was found to increase linearly with increasing particle concentration. An optimum concentration of 1 wt % was used to attain a maximum emission intensity. The observed fluorescence as an indication of the presence of dye-tagged polymer particles inside the organism has been scrutinized due to the ability of the hydrophilic fluorescent dye to leach into the medium from the polymer particles.[44,48] In order to rule out such incidences in the current investigation, a leaching test was performed for the prepared PMMA nanoparticles using a dialysis membrane experiment based on a reported method.[44] Full details are given in the experimental section. The PMMA used in the nanoparticle preparation had an average molecular weight of 15 kDa and thus is not able to pass through the dialysis membrane (a 3500 Da molecular weight cutoff). However, the perylene fluorophore with a molecular weight of 252.3 Da should be able to leach through the pores of the dialysis membrane. No appreciable fluorescence was detected in the leachate after 72 h compared to the control (Figure S1E), indicating that leaching of the hydrophobic perylene fluorophore from PMMA nanoparticles was minimal or insufficient to cause interference during imaging under confocal microscopy.

It is possible that the aqueous leaching environment tested may not be representative of the biological matrix that the ingested polymer nanoparticles are subjected to. However, this is difficult to study because a wide range of hydrophobic and hydrophilic environments exist in physiological environments.

Current criticisms of the use of fluorescence as an indicator of polymer nanoparticles use either water-soluble fluorophores[48] or the fluorophores merely surface-adsorbed on the particle.[44] This increases the chances of the fluorophore leaching or desorbing from the particle and represents the worst-case scenarios in which fluorophores could leach from polymer nanoparticles. However, the perylene fluorophore used in this study is insoluble in water and encapsulated within the PMMA matrix.[34] Fluorescence from the fluorophore was not observed to stain biological tissues, but they remain in clusters where the PMMA nanoparticles are adsorbed (Figure 1C). Therefore, it is concluded that the observed fluorescence originated from fluorophore-encapsulated polymer particles and not from leached perylene fluorophores.

As demonstrated in our previous studies, the PMMA nanoparticles produced via nanoprecipitation were observed to be stable over a period of 6 months,[14,34] and the PMMA nanoparticles were not toxic to *A. amphitrite* nauplii.[33] Sodium dodecylsulfate used for PMMA nanoparticle stabilization has a theoretical concentration far lower than the threshold at which cell viability is affected.[49] The PMMA nanoparticles formed polydispersed aggregates in filtered seawater with a size of 1.92 μm (Figure S1F). This is consistent with other literature observations of anionic polymer nanoparticles forming aggregates when dispersed in seawater.[12,50,51]

Although nanoscale plastic particles are predicted to occur in the pg/L to μg/L range in the environment,[7] the model organisms in the present study were exposed to a higher concentration because it is expected that only a fraction of the particles assimilated by the adult organisms are transferred to the offspring after losses by the exposed adult organisms through egestion and moulting.[14] The detection limit of confocal microscopy is relatively high due to interference from autofluorescence and background noise.[48,52] It was hence necessary to ensure that any maternally transferred PMMA nanoparticles are present at a detectable concentration and yet not at such a high concentration that adversely affects survival and reproduction.

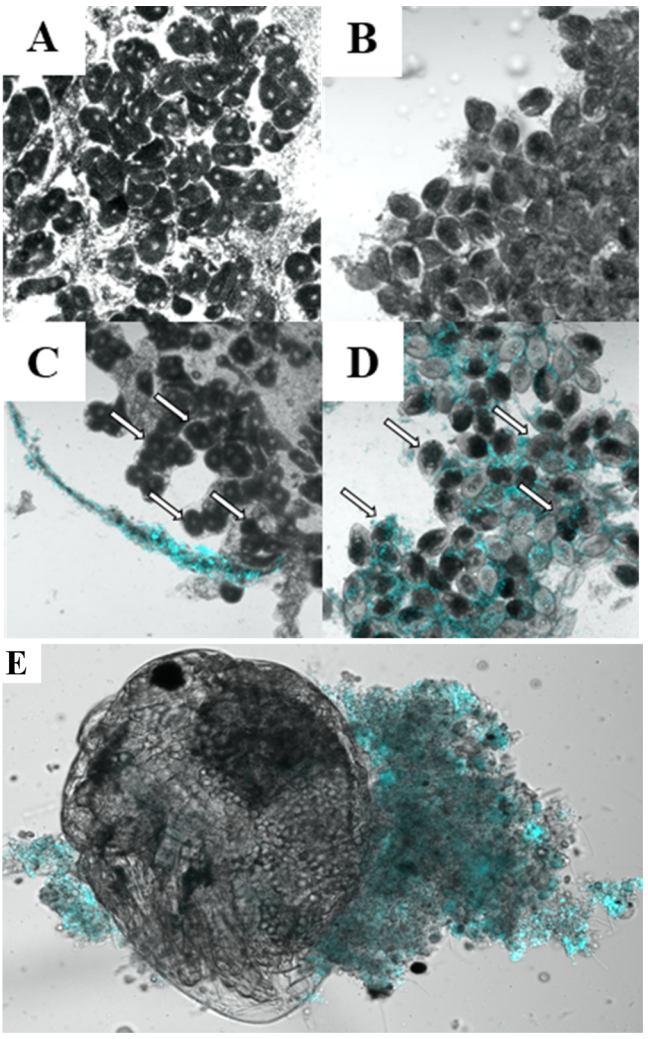

Figure 1. Confocal micrographs of the control (A,B) and PMMA particle-exposed adults (C,D), comprising bright-field images overlaid with confocal DAPI fluorescence images. Oocytes present within sub-mantle tissues of control adults (A) and adults exposed to PMMA nanoparticles (C). Developing embryos in egg lamellae from control adults (B) and adults exposed to PMMA nanoparticles (D). White arrows in (C,D) show the locations of a few oocytes (C) and embryos (D). An enlarged optical microscopy image (E) of a single nonfluorescent developing nauplius with surrounding tissues contaminated with fluorescent PMMA nanoparticles. The excitation wavelength (405 nm) and the detection wavelength (430−470 nm) corresponding to the perylene dye were used to detect the PMMA nanoparticles. Additional micrographs are given in Figures S2 and S3.

Translocation of PMMA Nanoparticles to *A. amphitrite* Sub-Mantle Tissues. A few papers exist in the literature describing the reproductive strategy used by barnacles.[53−56] Insemination by neighboring barnacles triggers the release of mature oocytes from sub-mantle tissues into an oviducal sac, and sperms enter the sac via surface pores to fertilize oocytes. Upon fertilization, a thin membrane arises to surround each embryo, and beneath this, an egg case develops subsequently.

https://doi.org/10.1021/acssuschemeng.1c01818
ACS Sustainable Chem. Eng. 2022, 10, 37−49

The oviducal sac encasing numerous developing embryos eventually moves to the bottom of the mantle cavity where it lies exposed to the respiratory current of the adult. This mass of embryos, also known as egg lamellae, is no longer metabolically connected to the adult, and it is from which stage II nauplii are hatched and released.

The ingression of oocytes by polymer nanoparticles can occur at any of these stages, and no such studies have been reported in the literature. Potentially, there are two major routes for introduction of PMMA nanoparticles into larvae, with the first being the true maternal transfer whereby ingested nanoparticles are deposited into oocytes during oogenesis and the second being passive absorption into developing embryos due to exposure to seawater laced with nanoparticles while egg lamellae were held inside mantle cavity.

The results suggested that maternal transfer of PMMA nanoparticles did not occur; PMMA nanoparticles were absent in oocytes and surrounding tissues from exposed parents (Figure 1A,C), indicating that PMMA nanoparticles were indeed absent in the sub-mantle tissues from the exposed adult. The only region detected with fluorescing nanoparticles was the ruptured membrane of the sub-mantle tissue removed from plastic exposed adults (Figure 1C) and was possibly due to absorption of nanoparticles from seawater drawn into mantle cavity. Nanoparticles were also found on moults shed from PMMA nanoparticle-exposed barnacles (data not presented), indicating that passive absorption can occur.

Barnacle feed using numerous appendages with fine hairs (cirri) to capture and retain particulates ranging from several millimeters to microns in size; these food particles are then transferred to mouthparts for maceration prior to ingestion. Analysis of stomach contents of *A. amphitrite* adults in Zhou Shan Sea revealed the predominant presence of organic detritus (2−4 μm) regardless of seasons.[57] It is possible that nanoparticles utilized in our study may be too small to be captured. Even if aggregate forms of PMMA nanoparticles (>1.9 μm) were caught, particulates could have been simply rejected at mouthparts or not assimilated after ingestion. Study with *Tetraclita squamosa* showed that animals could separate food from non-nutritious materials and reject the latter.[58] Early work with *Austrominius modestus* showed that inert particles consumed were mostly defecated in undigested state,[59] and Bhargava et al. demonstrated that larvae of *A. amphitrite* were capable of egesting PMMA nanoparticles (≈185 nm) in fecal excrements.[14] Despite exposure to extremely high concentrations of PMMA nanoparticles over 3 weeks, we could only speculate that perhaps the nanoparticles were not assimilated or not ingested at all in the absence of evidence supporting maternal transfer or any form of translocation (which was not investigated in this study).

It was also noted that embryos failed to show any uptake, although egg lamellae were exposed to PMMA nanoparticles drawn into mantle cavity (Figure 1D). Each barnacle embryo is effectively enclosed in three layers with the oviducal sac being the outermost and the first barrier against nanoparticle penetration. Surface pores present on the *A. amphitrite* oviducal sac could have facilitated entry of 167 nm PMMA nanoparticles in the present study, given that the pore size is on average 400−500 nm in temperate balanoide barnacles.[55,60] However, studies with zebrafish (*D. rerio*) embryos have shown otherwise. Kang et al. demonstrated that only 50 nm PS nanoparticles could pass through 500 nm pores on the chorion, but aggregates of 100 and 200 nm PS nanoparticles were blocked on the surface.[61] As observed in Figure 1D,E, PMMA nanoparticles presented as discrete clusters appeared to be absorbed onto the surface of the proteinaceous oviducal sac. Hence, it is likely that in the present study, aggregates of PMMA nanoparticles were physically excluded from entry via surface pores on the oviducal sac of *A. amphitrite*. Nevertheless, recent work revealed that nanoparticles failing to penetrate embryos could still impact larvae development by affecting the patency of embryos and leading to developmental toxicity.[62] Such factors will need to be examined using the nauplii in the near future.

Particle fluorescence observed on the sub-mantle tissues was also concentrated in discrete clusters on the exterior proteinaceous oviducal sac of the barnacle embryo (Figure 1E). In the event that the fluorophore leaches, we expect that the tissues contaminated with the fluorescent dye will show fluorescence, caused by direct dying by the leached fluorophore, which was not observed to be the case. Fluorescence from the barnacle specimens was mostly constricted to discrete clusters and locations (Figure 1C,D). Fluorescence was also absent inside the proteinaceous oviducal sac (Figure 1E), which suggests that it can physically exclude aggregates of fluorescent PMMA nanoparticles. In related experiments, human cells that were exposed to polymer particles showed discrete fluorescence from particles inside the cells.[63,64] Such results show that the observed fluorescence was localized within PMMA nanoparticle aggregates, hence indicating that the encapsulated fluorophore did not leach from the PMMA nanoparticles.

Maternal Transfer of Polymer Nanoparticles to Gametes in *S. bakau*. Full details of exposure conditions are given in the Methods and Materials. The eggs collected from PMMA nanoparticle-exposed and unexposed *S. bakau* adults were imaged under identical conditions (DAPI filter, ex/em 405/430−455 nm, Figures 3 and S2). Unfertilized eggs released from unexposed adult tubeworms were not fluorescent (Figure 2A, average emission intensity = 6.462×10^5, SD = 6.181×10^4), while eggs collected from animals exposed to PMMA nanoparticles were significantly more fluorescent (Figure 2B, average emission intensity = 1.294×10^7, SD = 2.376×10^6), $t(11) = -12.50$, $p < 0.00001$). This shows the presence of PMMA nanoparticles inside the eggs collected from adult tubeworms exposed to PMMA nanoparticles. This is very different from what is described for the case of *A. amphitrite* eggs and developing embryos, both of which did not contain any fluorescent particles. In addition, the contents from lysed eggs from adults not exposed to particles showed no fluorescence (Figure 2C), and the lysed eggs from particle-exposed tubeworms leaked their fluorescent content (Figure 2D). The presence of PMMA nanoparticles inside the eggs was confirmed by the cross-sectional imaging of eggs collected from adults exposed to luminescent PMMA nanoparticles using *z*-stack imaging (Figure 3). The cross-sectional images in Figure 3B−E showed that fluorescence from the dye-tagged PMMA nanoparticles originates mostly from inside the egg. Hence, it is concluded that the fluorescent PMMA nanoparticles were present inside the egg. Other detailed DAPI and bright-field micrographs are given in the Supporting Information, Figure S5. The presence of PMMA nanoparticles inside the unfertilized transparent eggs collected from exposed adults suggests that the particles ingested by the *S. bakau* adult worms could have been transferred to their eggs during oogenesis. Similar to their congeners,[65,66] oogenesis in the *S.*

https://doi.org/10.1021/acssuschemeng.1c01818
ACS Sustainable Chem. Eng. 2022, 10, 37−49

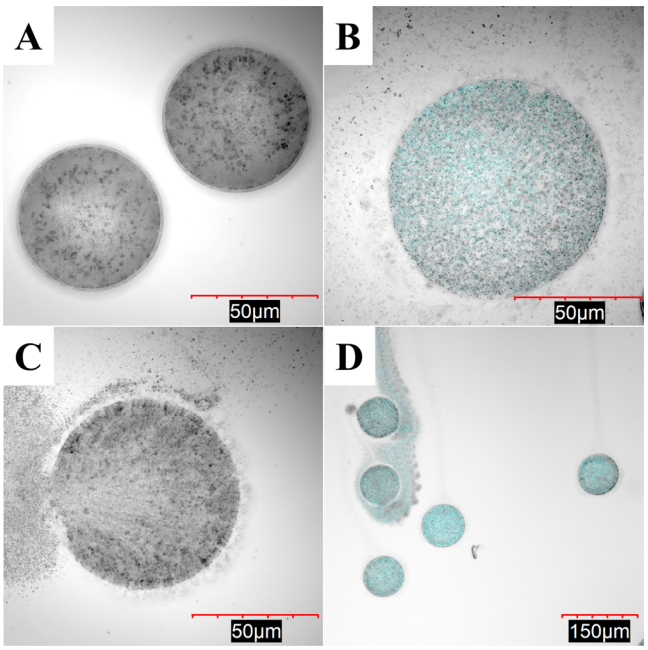

Figure 2. Confocal micrographs of freshly released tubeworm eggs, comprising a differential interference contrast image overlaid with the fluorescence image (A–D). Eggs from the unexposed, control animals (A) and eggs collected from adult worms exposed to PMMA particles recorded under identical imaging conditions (B). A control egg was found to release nonfluorescent lysate (C), while the lysate from eggs collected from animals exposed to particles was fluorescent (D). DAPI and bright-field micrographs are given in Figure S4.

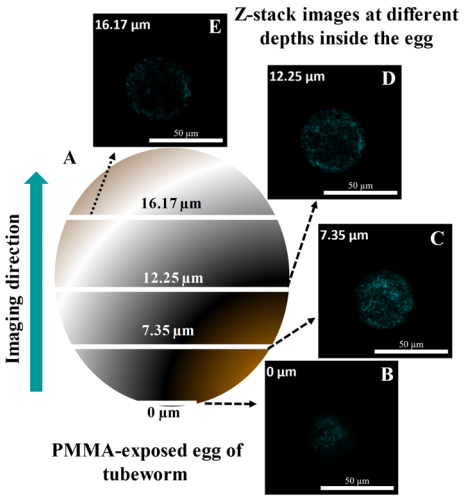

Figure 3. Schematic representation of a *S. bakau* egg (A), with confocal *z*-stack slices at 0 (B), 7.35 (C), 12.25 (D), and 16.17 μm (E), collected from adults exposed to PMMA nanoparticles. The egg has a typical radius of circa 50 μm. The scale bars (50 μm) in all micrographs are kept the same for comparison.

bakau worms used in this study may be extraovarian, that is, eggs are released from ovaries in the pre-vitellogenic phase and undergo vitellogenesis in the coelomic cavity.[67,68] Vitellogenesis marks the onset of yolk deposition inside the developing eggs with the incorporation of yolk precursors or proteins from the celomic fluid, assuming the presence of heterosynthetic pathways for the formation of yolk. Vitellogenesis typically takes place over a prolonged duration due to the time needed for the eggs to accumulate all necessary components to attain full viability.[65−67] It is plausible that the PMMA nanoparticles present in the coelomic fluid get transferred into the eggs during this process. Further studies are needed to confirm the presence of such a transfer mechanism in *S. bakau* tubeworms.

Previous research has established that certain proteins adsorb on the surface of nanoparticles when they are introduced in biological fluids such as serum or plasma, forming a biological interface known as the protein corona.[69] Yolk precursor proteins such as vitellogenin have been demonstrated to be incorporated into the protein coronae around the nanoparticles.[70,71] Having a large molecular weight, vitellogenin is generally known to enter polychaete eggs via receptor-mediated endocytosis.[68,72] Thus, it is possible that the protein corona formed around the PMMA nanoparticles in the celomic fluid mediated the uptake of PMMA into eggs by virtue of harboring proteins recognizable by receptors on the cell membrane of the tubeworm eggs.[13,73] This hypothesis needs to be explored further in a future study by profiling the protein corona formed around PMMA nanoparticles in female *S. bakau* tubeworms. In addition, other nonendocytic routes of entry, such as passive penetration through the cell membrane or through membrane pores that may allow the passage of the PMMA nanoparticles based on particle size and charge, should also be investigated.[74−76]

A highly magnified confocal micrograph of a blastula developed from eggs collected from PMMA nanoparticle-exposed adults showed that the fluorescence originates from localized discrete packets (Figure 4A–C). As explained earlier, yolk precursor proteins such as vitellogenin[67] could have mediated the uptake of PMMA nanoparticles into the eggs during vitellogenesis.[13] Similar to the reported case of maternal transfer in the zebra fish model,[13] we postulate that the discrete fluorescent packets correspond to yolk storage granules, where the hydrophobic PMMA nanoparticles could have localized.

Development of *S. bakau* Embryos. Eggs from both PMMA nanoparticle-exposed and unexposed *S. bakau* adults were fertilized, incubated, and allowed to develop for understanding the maternal transfer of nanoplastics (Figures 5 and S5). Even though the eggs collected from PMMA-exposed adults showed intense fluorescence, the trochophores hatched (17 hpf) from the fluorescent eggs showed low emission intensity, similar to the trochophores (17 hpf) from control eggs (Figure 6). This is interesting considering that the PMMA nanoparticles seem to be egested by the embryo during the development. To determine the fate of the polymer nanoparticles in the developing *S. bakau* embryos, a few stages of embryonic development were sampled and imaged using a confocal microscope. The 0.5 hpf cell division stage of the freshly fertilized eggs (Figures 5A and 6) was still as fluorescent as the unfertilized eggs collected from adults exposed to PMMA nanoparticles (Figure 5A), while the fluorescence emission intensity from embryos at the 7 hpf rotating blastula stage (Figure 5B) dropped to 39% of the original intensity exhibited by the unfertilized eggs. The trochophores (17 hpf, Figure 5C) hatched from luminescent eggs were practically nonemissive in nature. It is remarkable to notice that fluorescence intensity gradually reduced with the advancing development of the fertilized eggs.

Interestingly, the average fluorescence intensities from each stage of development of the eggs collected from exposed adults decreased exponentially with increasing time (Figure 6). At 5 hpf, the blastula showed a decrease of 61% in fluorescence, and

https://doi.org/10.1021/acssuschemeng.1c01818
ACS Sustainable Chem. Eng. 2022, 10, 37−49

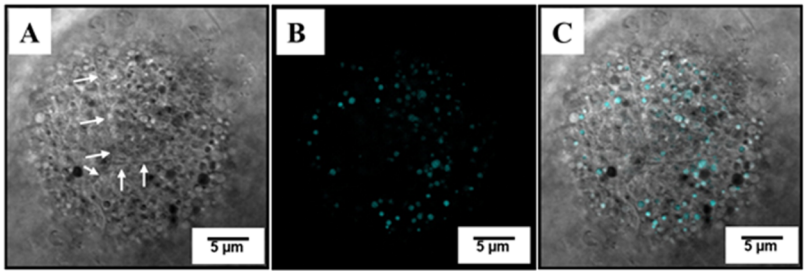

Figure 4. Highly magnified confocal micrograph of the eggs showing the boundaries between blastomeres in the blastula, as indicated by the white arrows (A) and the distribution of fluorescent particles inside the egg using the DAPI mode (B). The overlaid image (C) shows fluorescence signals distributed within the blastomeres in *S. bakau* blastula.

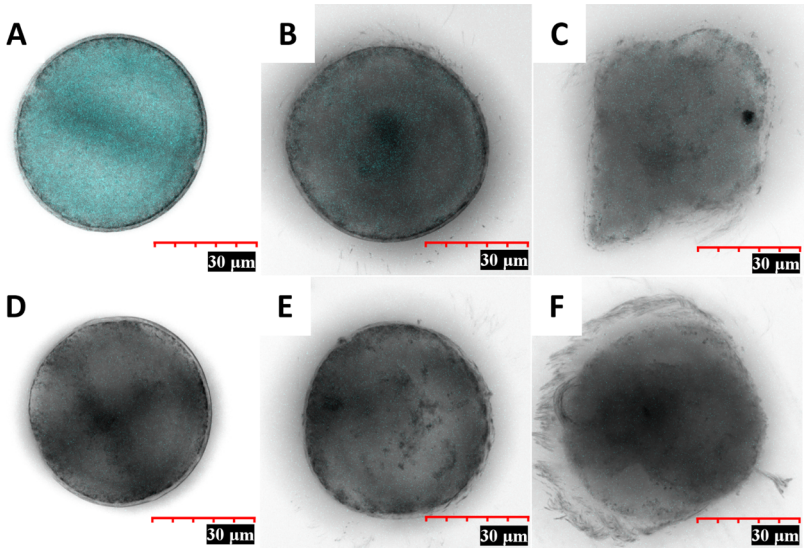

Figure 5. Confocal micrographs of developing *S. bakau* eggs collected from exposed (A–C) and unexposed (D–F) adults at the beginning of the cell division stage [0.5 hpf, (A,D)] at the rotating blastula stage [7 hpf, (B,E)] and the trochophore stage [17 hpf, (C,F)]. The scale bars in all images are maintained the same for comparison. Other detailed DAPI and bright-field micrographs are given in the Supporting Information (Figure S6).

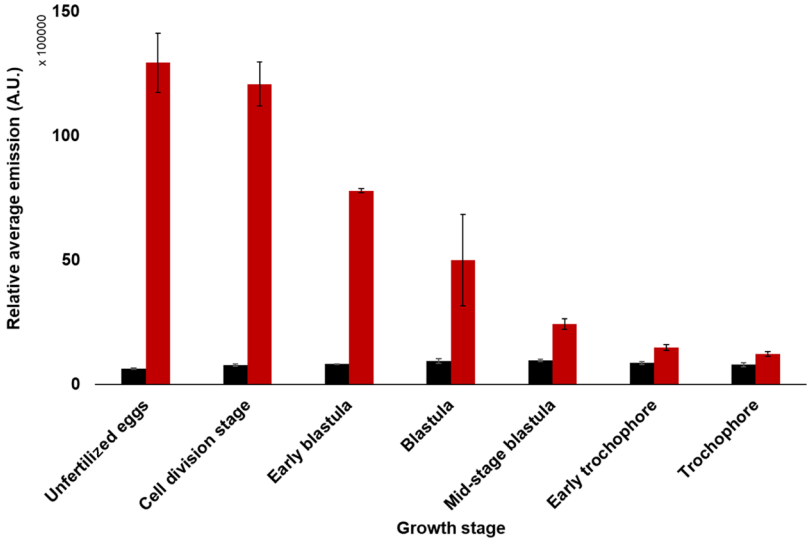

Figure 6. Fluorescence intensities of eggs collected from adults not exposed (■, natural background fluorescence) and exposed (red ■) to PMMA nanoparticles. Integrated fluorescence intensities were taken from a minimum of 21 eggs each, from PMMA-exposed parents and from unexposed parents, which were analyzed during these seven stages of development in the span of 17 h.

the developed trochophores after 17 hpf had lost 91% of the original fluorescence intensity. This interesting exponential decay of the average fluorescence (Figure 6) and the intracellular location of the particles suggest that there exists

https://doi.org/10.1021/acssuschemeng.1c01818
ACS Sustainable Chem. Eng. 2022, 10, 37–49

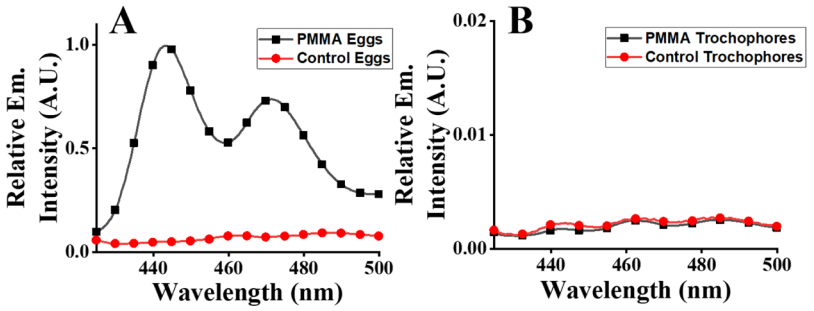

Figure 7. Fluorescence spectra from unfertilized eggs (A) from PMMA nanoparticle-exposed parents (−■−) and unexposed parents (red −●−) and trochophores [24 hpf, (B)] from exposed parents (−■−) and unexposed parents (red −●−). The eggs and trochophores sampled were digested in hydrogen peroxide solution before the PMMA nanoparticles were extracted using DCM, from which the emission spectra were obtained. Plot (B) has been magnified along the vertical axis to aid in visualization as the emission spectra were very weak. The spectrum from the positive control sample is given in the Supporting Information (Figure S7).

a mechanism for ejecting the polymer particles during the development of the embryos into trochophores.

Release of Fluorescent Polymer Nanoparticles via Exocytosis. The exocytosis pathway(s) through which PMMA nanoparticles could be released from the developing *S. bakau* embryos is largely dependent on their uptake pathways and fate after entry into the eggs. Behazadi et al. outlined various pathways along which endocytosed nanoparticles can travel within a cell before being released into the extracellular environment.[75] Following uptake, nanoparticles are typically delivered to early endosomes where they undergo sorting according to their different intracellular destinations. While some nanoparticles are released intact from the cells, others may be directed toward lysosomal degradation before release. Synthetic polymers such as PMMA have no known degradation pathway inside the cells. After entry, the PMMA nanoparticles were evidently retained within the eggs till fertilization, which once again points to our hypothesis that the nanoparticles were likely to have been localized within the yolk storage granules. Since yolk is stored in the granules till use by the developing embryo, it follows that the PMMA nanoparticles were not immediately directed toward a release pathway till the onset of fertilization and embryonic development. During embryogenesis, yolk reserves start to be gradually utilized by the developing embryos. This process could have facilitated the release of the PMMA nanoparticles from the embryos via an exocytosis mechanism. The protein corona adsorbed onto the surfaces of the nanoparticles could have also been subjected to compositional changes that led to their targeted release from the eggs. Exocytosis of nanoparticles from various cells has been studied by many research groups and reported in the literature.[77,78] Since the exocytosis happens favorably, some nanoparticles used in drug delivery applications are engineered specifically to reduce or control exocytosis of particles from cells.[77,79] Moreover, the rate of exocytosis of nanoparticles from cells is also influenced by the physiochemical properties of the nanoparticles such as their surface charges, with negatively charged nanoparticles undergoing faster exocytosis than positively charged particles.[77,80] The PMMA nanoparticles used in our study also possess a negative surface charge of −28.4 mV (Figure S1F).[34] The intracellular fate of the PMMA nanoparticles and their exocytosis pathways from developing embryos should be investigated further in a separate study.

Fluorophore Extraction from Developing *S. bakau* Eggs. To further explore the mechanism of disappearance of fluorescence from developing eggs, the following experiments were performed: we explored the possibility that instead of egestion, the observed loss of the fluorescence signal was caused by quenching of fluorescence through an intracellular mechanism. In this scenario, the fluorophore and polymer are expected to remain inside the trochophores after 24 hpf. However, if the particles were egested by the developing eggs into the water column, no particles or fluorescent dye should be observed inside the eggs. In order to test this hypothesis, a sub-sample of the unfertilized eggs and trochophores were digested separately with hydrogen peroxide and extracted with an organic solvent, DCM, to check for the presence of the PMMA nanoparticles and fluorophore inside the cells. Here, we followed a reported protocol for the extraction of polymer particles from biological samples.[81−83] The DCM extracts from the digested solution of unfertilized eggs collected from adults exposed and unexposed to PMMA particles are given in Figure 7A. The extract from unfertilized eggs collected from the adults exposed to polymer nanoparticles showed strong fluorescence emission at 448 and 476 nm, matching the emission spectrum of the perylene dye encapsulated inside the polymer nanoparticles (Figure 7A). The fluorescence spectra of the extract from trochophores obtained from eggs of exposed and unexposed adults showed no fluorescence after 24 hpf (Figure 7B), indicating a complete egestion of polymer particles from trochophores. These results are complementary to the results obtained from confocal microscopic investigations described in Figure 5, indicating the absence of particles in trochophores hatched from eggs with PMMA nanoparticles. The DCM extract from a positive control involving perylene-encapsulated PMMA nanoparticles dispersed in water exhibited similar emission properties and was used for comparison (Figure S7).

Effect of Maternally Transferred PMMA Nanoparticles on *S. bakau* Larval Development. Even though the trochophores from exposed tubeworm parents at 24 hpf do not contain any PMMA nanoparticles, the initial stages of fertilized eggs contained a substantial number of polymer nanoparticles. This warrants the question on what the consequences are, if any, on the development of the trochophores. To understand the dormant effects of exposure of PMMA nanoplastics on the first-generation larvae from exposed parents, the development and settlement of the trochophores from exposed and unexposed tubeworms were quantified and compared over a period of 10 days. In all samples, there were between 2 and 12% of trochophores with an abnormal morphology on average. Morphological abnormalities exhibited by trocho-

https://doi.org/10.1021/acssuschemeng.1c01818
ACS Sustainable Chem. Eng. 2022, 10, 37−49

phores included an enlarged digestive tract and a round-shaped terminal region (Figure S8A−C), whereas normal healthy trochophores have an overall conical shape with a tapered and pointed terminal region (Figure S8D). It was noted that the percentage of trochophores with an abnormal morphology did not differ significantly between trochophores reared from adults exposed or unexposed to PMMA nanoparticles. The average proportion of trochophores with a normal morphology across the duration of the experiment was 96% (SD = 3.357) for those from exposed parents and 97% (SD = 2.907) for trochophores from unexposed parents, indicating that there were no significant differences in development between offspring from PMMA nanoparticle-exposed parents and unexposed parents at a significance level <0.05, $t(19) = 0.410$, $p = 0.343$ (Figure S8E). The difference in settlement rates between the two treatment groups was also not statistically significant at $p < 0.05$, $t(19) = 0.027$, $p = 0.490$ (Figure S8F). Trochophores from PMMA nanoparticle-exposed parents had an average settlement of 22% (SD = 29.304) after 10 days, while trochophores from unexposed parents had an average settlement of 23% (SD = 26.760). Hence, it is concluded that PMMA nanoparticle exposure during the egg development phase did not affect subsequent larval development.

Comparison of Maternal Transfer of PMMA Nanoparticles in *A. amphitrite* and *S. bakau*. The two species of different phyla, *A. amphitrite* and *S. bakau*, investigated in this study for their potential to ingest and maternally transfer PMMA nanoparticles to their offspring, were found to have different mechanisms for mitigating the exposure and transfer risks of PMMA nanoparticles to offspring. The two species were exposed to the same batches of PMMA nanoparticles (e.g., size and surface charges) under similar exposure conditions (e.g., concentration). Exposed *A. amphitrite* adults did not transfer the PMMA nanoparticles to developing eggs, even though such luminescent particles were observed on their sub-mantle tissues. On the other hand, eggs collected from *S. bakau* adults exposed to PMMA nanoparticles contained the luminescent PMMA nanoparticles, but the resultant offspring were particle-free.

It is evident that reproduction in *A. amphitrite* is less susceptible to interference by the PMMA nanoparticles as compared to that in *S. bakau* due to their inherent physiological differences. The size of nanoparticles appeared to be a critical consideration in terms of translocation as smaller particles (≤50 nm) have been shown to successfully cross the chorion barrier in zebrafish embryos.[13,61] In another study however, nematodes were shown to maternally transfer 100 nm PS nanoparticles,[19] suggesting that animal models used should also be taken into account given the differences in biological makeup and cellular processes at the various trophic levels. In both animal models investigated here, the offspring are protected from contamination of the PMMA nanoparticles through different mechanisms. Such results are in fact encouraging toward understanding the biological mechanism that protects the overall health of offspring and the ecosystem.

Although *A. amphitrite* has shown in this study to disallow maternal transfer of PMMA nanoparticles, another study reported that exposure to PS microbeads at 1000 beads/mL produced progeny with significantly increased larval mortality and a reduced development rate.[84] It would be interesting to study and compare such transgenerational effects of exposure to nanoparticles of various common polymers in different marine organisms. Another plausible route for transfer of nanoplastics to the offspring of exposed animals may be via spermatozoa. Although PS nanoparticles do not enter the spermatozoa cells from *D. rerio*[13] and *Crassostrea gigas*,[85] it is possible that the potential for such transfer may exist in different species.

CONCLUSIONS

Two animal models with different reproduction strategies were exposed to fluorescent PMMA nanoparticles under similar conditions to understand the process of maternal transfer of nanoplastics. The PMMA nanoparticles prepared in the lab were fully characterized and showed no fluorophore leaching under experimental conditions used in this study. In addition, the fluorescence observed under a confocal microscope showed discrete emission from PMMA nanoparticles inside the eggs and embryos. *A. amphitrite* embryos appeared to be void of the PMMA nanoparticles, although aggregates of fluorescent nanoparticles were found on the egg case surrounding the embryos. The results indicate that no maternal transfer of PMMA nanoparticles occurred to the eggs or embryos of *A. amphitrite*. On the other hand, eggs released from exposed *S. bakau* adults contained fluorescent PMMA nanoparticles confined to yolk granules or vacuoles inside the eggs. Fluorescence emission from the fertilized developing embryo decreased gradually, and no emission was observed from the trochophore (24 hpf). The PMMA nanoparticles were released from the developing embryo through exocytosis, and the resultant trochophores did not show significant changes in morphology or impaired development when compared to those trochophores from control parents.

Our findings suggest that different animals have various coping mechanisms to mitigate exposure to nanoplastics or other pollutants, as observed in the case of *A. amphitrite* and *S. bakau*. This implies that future investigations should be cautious toward drawing general conclusions when testing single animal models in isolation. Although *A. amphitrite* and *S. bakau* did not maternally transfer PMMA nanoparticles to their progenies, particles of other polymers with different sizes and additives may have different potential for maternal transfer and therefore should be tested in the future to understand the impact of nanoplastics and microplastics pollution on living organisms.

ASSOCIATED CONTENT

Supporting Information

The Supporting Information is available free of charge at https://pubs.acs.org/doi/10.1021/acssuschemeng.1c01818.

PMMA nanoparticle characterization data; DAPI, bright-field, and overlaid micrographs; emission spectrum for particles extracted using DCM; and data for the trochophore morphology and settlement study (PDF)

AUTHOR INFORMATION

Corresponding Authors

Serena Lay-Ming Teo − *St. John's Island National Marine Laboratory, Tropical Marine Science Institute, National University of Singapore, Singapore 119227, Singapore*; Email: tmsteolm@nus.edu.sg

Suresh Valiyaveettil − *Department of Chemistry, National University of Singapore, Singapore 117543, Singapore;*

orcid.org/0000-0001-6990-660X; Email: chmsv@nus.edu.sg

Authors

Yong Jie Yip − *Department of Chemistry, National University of Singapore, Singapore 117543, Singapore*

Gayathiri D/O Sivananthan − *St. John's Island National Marine Laboratory, Tropical Marine Science Institute, National University of Singapore, Singapore 119227, Singapore*

Serina Siew Chen Lee − *St. John's Island National Marine Laboratory, Tropical Marine Science Institute, National University of Singapore, Singapore 119227, Singapore*

Mei Lin Neo − *St. John's Island National Marine Laboratory, Tropical Marine Science Institute, National University of Singapore, Singapore 119227, Singapore*

Complete contact information is available at: https://pubs.acs.org/10.1021/acssuschemeng.1c01818

Notes

The authors declare no competing financial interest.

■ ACKNOWLEDGMENTS

The authors acknowledge funding support from the National Research Foundation Singapore for research conducted under the Marine Science R&D Program (MSRDP-P07) at St. John's Island National Marine Laboratory. Part of this research is also supported by the National Research Foundation, Singapore, under its NRF-NERC-SEAP-2020-04 (WBS no. R-143-000-B72-281). The authors wish to thank the Department of Chemistry and St. John's Island National Marine Laboratory for providing the necessary facility support toward this research.

■ REFERENCES

(1) Zhang, R.; Silic, M. R.; Schaber, A.; Wasel, O.; Freeman, J. L.; Sepúlveda, M. S. Exposure Route Affects the Distribution and Toxicity of Polystyrene Nanoplastics in Zebrafish. *Sci. Total Environ.* **2020**, *724*, 138065.

(2) Sökmen, T. Ö.; Sulukan, E.; Türkoğlu, M.; Baran, A.; Özkaraca, M.; Ceyhun, S. B. Polystyrene Nanoplastics (20 Nm) Are Able to Bioaccumulate and Cause Oxidative DNA Damages in the Brain Tissue of Zebrafish Embryo (Danio Rerio). *Neurotoxicology* **2020**, *77*, 51−59.

(3) Abarghouei, S.; Hedayati, A.; Raeisi, M.; Hadavand, B. S.; Rezaei, H.; Abed-Elmdoust, A. Size-Dependent Effects of Microplastic on Uptake, Immune System, Related Gene Expression and Histopathology of Goldfish (Carassius Auratus). *Chemosphere* **2021**, *276*, 129977.

(4) Yu, C.-W.; Luk, T. C.; Liao, V. H.-C. Long-Term Nanoplastics Exposure Results in Multi and Trans-Generational Reproduction Decline Associated with Germline Toxicity and Epigenetic Regulation in Caenorhabditis Elegans. *J. Hazard. Mater.* **2021**, *412*, 125173.

(5) Chamas, A.; Moon, H.; Zheng, J.; Qiu, Y.; Tabassum, T.; Jang, J. H.; Abu-Omar, M.; Scott, S. L.; Suh, S. Degradation Rates of Plastics in the Environment. *ACS Sustainable Chem. Eng.* **2020**, *8*, 3494−3511.

(6) Bruyninckx, K.; Dusselier, M. Sustainable Chemistry Considerations for the Encapsulation of Volatile Compounds in Laundry-Type Applications. *ACS Sustainable Chem. Eng.* **2019**, *7*, 8041−8054.

(7) Lenz, R.; Enders, K.; Nielsen, T. G. Microplastic Exposure Studies Should Be Environmentally Realistic. *Proc. Natl. Acad. Sci. U.S.A.* **2016**, *113*, E4121−E4122.

(8) Andrady, A. L. Microplastics in the Marine Environment. *Mar. Pollut. Bull.* **2011**, *62*, 1596−1605.

(9) GESAMP. Sources, Fate and Effects of Microplastics in the Marine Environment: A Global Assessment. Working Group 40. 2nd Phase. *Rep. Stud. - GESAMP* **2017**, *90*, 220.

(10) Gigault, J.; Halle, A. t.; Baudrimont, M.; Pascal, P.-Y.; Gauffre, F.; Phi, T.-L.; El Hadri, H.; Grassl, B.; Reynaud, S. Current Opinion: What Is a Nanoplastic? *Environ. Pollut.* **2018**, *235*, 1030−1034.

(11) Fu, W.; Min, J.; Jiang, W.; Li, Y.; Zhang, W. Separation, Characterization and Identification of Microplastics and Nanoplastics in the Environment. *Sci. Total Environ.* **2020**, *721*, 137561.

(12) Bergami, E.; Bocci, E.; Vannuccini, M. L.; Monopoli, M.; Salvati, A.; Dawson, K. A.; Corsi, I. Nano-Sized Polystyrene Affects Feeding, Behavior and Physiology of Brine Shrimp Artemia Franciscana Larvae. *Ecotoxicol. Environ. Saf.* **2016**, *123*, 18−25.

(13) Pitt, J. A.; Trevisan, R.; Massarsky, A.; Kozal, J. S.; Levin, E. D.; Di Giulio, R. T. Maternal Transfer of Nanoplastics to Offspring in Zebrafish (Danio Rerio): A Case Study with Nanopolystyrene. *Sci. Total Environ.* **2018**, *643*, 324−334.

(14) Bhargava, S.; Chen Lee, S. S.; Min Ying, L. S.; Neo, M. L.; Lay-Ming Teo, S.; Valiyaveettil, S. Fate of Nanoplastics in Marine Larvae: A Case Study Using Barnacles, Amphibalanus Amphitrite. *ACS Sustainable Chem. Eng.* **2018**, *6*, 6932−6940.

(15) Jeong, C.-B.; Won, E.-J.; Kang, H.-M.; Lee, M.-C.; Hwang, D.-S.; Hwang, U.-K.; Zhou, B.; Souissi, S.; Lee, S.-J.; Lee, J.-S. Microplastic Size-Dependent Toxicity, Oxidative Stress Induction, and p-JNK and p-P38 Activation in the Monogonont Rotifer (Brachionus Koreanus). *Environ. Sci. Technol.* **2016**, *50*, 8849−8857.

(16) Mattsson, K.; Johnson, E. V.; Malmendal, A.; Linse, S.; Hansson, L.-A.; Cedervall, T. Brain Damage and Behavioural Disorders in Fish Induced by Plastic Nanoparticles Delivered through the Food Chain. *Sci. Rep.* **2017**, *7*, 1−7.

(17) Yu, S.-P.; Cole, M.; Chan, B. K. K. Effects of Microplastic on Zooplankton Survival and Sublethal Responses. *Oceanogr. Mar. Biol.* **2020**, *58*, 359−408.

(18) Yu, S.-P.; Nakaoka, M.; Chan, B. K. K. The Gut Retention Time of Microplastics in Barnacle Naupliar Larvae from Different Climatic Zones and Marine Habitats. *Environ. Pollut.* **2021**, *268*, 115865.

(19) Zhao, L.; Qu, M.; Wong, G.; Wang, D. Transgenerational Toxicity of Nanopolystyrene Particles in the Range of Mg L-1 in the Nematode: Caenorhabditis Elegans. *Environ. Sci.: Nano* **2017**, *4*, 2356−2366.

(20) Collard, F.; Gilbert, B.; Compère, P.; Eppe, G.; Das, K.; Jauniaux, T.; Parmentier, E. Microplastics in Livers of European Anchovies (Engraulis Encrasicolus , L.). *Environ. Pollut.* **2017**, *229*, 1000−1005.

(21) Lu, Y.; Zhang, Y.; Deng, Y.; Jiang, W.; Zhao, Y.; Geng, J.; Ding, L.; Ren, H. Uptake and Accumulation of Polystyrene Microplastics in Zebrafish (Danio Rerio) and Toxic Effects in Liver. *Environ. Sci. Technol.* **2016**, *50*, 4054−4060.

(22) Kolandhasamy, P.; Su, L.; Li, J.; Qu, X.; Jabeen, K.; Shi, H. Adherence of Microplastics to Soft Tissue of Mussels: A Novel Way to Uptake Microplastics beyond Ingestion. *Sci. Total Environ.* **2018**, *610−611*, 635−640.

(23) Barboza, L. G. A.; Vieira, L. R.; Branco, V.; Figueiredo, N.; Carvalho, F.; Carvalho, C.; Guilhermino, L. Microplastics Cause Neurotoxicity, Oxidative Damage and Energy-Related Changes and Interact with the Bioaccumulation of Mercury in the European Seabass, Dicentrarchus Labrax (Linnaeus, 1758). *Aquat. Toxicol.* **2018**, *195*, 49−57.

(24) Détrée, C.; Gallardo-Escárate, C. Polyethylene Microbeads Induce Transcriptional Responses with Tissue-Dependent Patterns in the Mussel Mytilus Galloprovincialis. *J. Molluscan Stud.* **2017**, *83*, 220−225.

(25) Sivananthan, G.; Shantti, P.; Kupriyanova, E. K.; Quek, Z. B. R.; Yap, N. W. L.; Teo, S. L. M. Spirobranchus Bakau Sp. Nov. from Singapore: Yet Another Species of S. Kraussii-Complex (Polychaeta: Serpulidae). *Zootaxa* **2021**, *5040*, 33−65.

(26) Chan, J. Y.-H.; Lee, S. S.-C.; Zainul Rahim, S. Z.; Teo, S. L.-M. Settlement Inducers for Larvae of the Tropical Fouling Serpulid,

Spirobranchus Kraussii (Baird, 1865) (Polychaeta: Annelida). *Int. Biodeterior. Biodegrad.* **2014**, *94*, 192−199.
(27) Baird, W. Description of Several New Species and Varieties of Tubicolous Annelides=Tribe Limivora of Grube, in the Collection of the British Museum. *J. Proc. Linn. Soc. London, Zool.* **1864**, *8*, 10−22.
(28) Jambeck, J. R.; Geyer, R.; Wilcox, C.; Siegler, T. R.; Perryman, M.; Andrady, A.; Narayan, R.; Law, K. L. Plastic Waste Inputs from Land into the Ocean. *Science* **2015**, *347*, 768−771.
(29) Luo, Y. Y.; Not, C.; Cannicci, S. Mangroves as Unique but Understudied Traps for Anthropogenic Marine Debris: A Review of Present Information and the Way Forward. *Environ. Pollut.* **2021**, *271*, 116291.
(30) Deng, H.; He, J.; Feng, D.; Zhao, Y.; Sun, W.; Yu, H.; Ge, C. Microplastics Pollution in Mangrove Ecosystems: A Critical Review of Current Knowledge and Future Directions. *Sci. Total Environ.* **2021**, *753*, 142041.
(31) Thomas, P. J.; Perono, G.; Tommasi, F.; Pagano, G.; Oral, R.; Burić, P.; Kovačić, I.; Toscanesi, M.; Trifuoggi, M.; Lyons, D. M. Resolving the Effects of Environmental Micro- and Nanoplastics Exposure in Biota: A Knowledge Gap Analysis. *Sci. Total Environ.* **2021**, *780*, 146534.
(32) Martin, C.; Baalkhuyur, F.; Valluzzi, L.; Saderne, V.; Cusack, M.; Almahasheer, H.; Krishnakumar, P. K.; Rabaoui, L.; Qurban, M. A.; Arias-Ortiz, A.; et al. Exponential Increase of Plastic Burial in Mangrove Sediments as a Major Plastic Sink. *Sci. Adv.* **2020**, *6*, No. eaaz5593.
(33) Yip, Y. J.; Lee, S. S. C.; Neo, M. L.; Teo, S. L.-M.; Valiyaveettil, S. A Comparative Investigation of Toxicity of Three Polymer Nanoparticles on Acorn Barnacle (Amphibalanus Amphitrite). *Sci. Total Environ.* **2022**, *806*, 150965.
(34) Bhargava, S.; Chu, J. J. H.; Valiyaveettil, S. Controlled Dye Aggregation in Sodium Dodecylsulfate-Stabilized Poly-(Methylmethacrylate) Nanoparticles as Fluorescent Imaging Probes. *ACS Omega* **2018**, *3*, 7663−7672.
(35) Mohamed Nor, N. H.; Obbard, J. P. Microplastics in Singapore's Coastal Mangrove Ecosystems. *Mar. Pollut. Bull.* **2014**, *79*, 278−283.
(36) Yu, S.-P.; Chan, B. K. K. Effects of Polystyrene Microplastics on Larval Development, Settlement, and Metamorphosis of the Intertidal Barnacle Amphibalanus Amphitrite. *Ecotoxicol. Environ. Saf.* **2020**, *194*, 110362.
(37) Venâncio, C.; Ferreira, I.; Martins, M. A.; Soares, A. M. V. M.; Lopes, I.; Oliveira, M. The Effects of Nanoplastics on Marine Plankton: A Case Study with Polymethylmethacrylate. *Ecotoxicol. Environ. Saf.* **2019**, *184*, 109632.
(38) Brandts, I.; Barría, C.; Martins, M. A.; Franco-Martínez, L.; Barreto, A.; Tvarijonaviciute, A.; Tort, L.; Oliveira, M.; Teles, M. Waterborne Exposure of Gilthead Seabream (Sparus Aurata) to Polymethylmethacrylate Nanoplastics Causes Effects at Cellular and Molecular Levels. *J. Hazard. Mater.* **2021**, *403*, 123590.
(39) Liu, H.; Tian, L.; Wang, S.; Wang, D. Size-Dependent Transgenerational Toxicity Induced by Nanoplastics in Nematode Caenorhabditis Elegans. *Sci. Total Environ.* **2021**, *790*, 148217.
(40) Billinton, N.; Knight, A. W. Seeing the Wood through the Trees: A Review of Techniques for Distinguishing Green Fluorescent Protein from Endogenous Autofluorescence. *Anal. Biochem.* **2001**, *291*, 175−197.
(41) Benson, R. C.; Meyer, R. A.; Zaruba, M. E.; McKhann, G. M. Cellular Autofluorescence–Is It Due to Flavins? *J. Histochem. Cytochem.* **1979**, *27*, 44−48.
(42) Qiu, J.; Qian, P. Tolerance of the Barnacle Balanus Amphitrite Amphitrite to Salinity and Temperature Stress:Effects of Previous Experience. *Mar. Ecol.: Prog. Ser.* **1999**, *188*, 123−132.
(43) Chou, R.; Lee, H. B. Commercial Marine Fish Farming in Singapore. *Aquacult. Res.* **1997**, *28*, 767−776.
(44) Catarino, A. I.; Frutos, A.; Henry, T. B. Use of Fluorescent-Labelled Nanoplastics (NPs) to Demonstrate NP Absorption Is Inconclusive without Adequate Controls. *Sci. Total Environ.* **2019**, *670*, 915−920.
(45) Gabilondo, R.; Graham, H.; Caldwell, G. S.; Clare, A. S. Laboratory Culture and Evaluation of the Tubeworm Ficopomatus Enigmaticus for Biofouling Studies. *Biofouling* **2013**, *29*, 869−878.
(46) Clancy, B.; Cauller, L. J. Reduction of Background Autofluorescence in Brain Sections Following Immersion in Sodium Borohydride. *J. Neurosci. Methods* **1998**, *83*, 97−102.
(47) Schelkle, K. M.; Schmid, C.; Yserentant, K.; Bender, M.; Wacker, I.; Petzoldt, M.; Hamburger, M.; Herten, D.-P.; Wombacher, R.; Schröder, R. R.; et al. Cell Fixation by Light-Triggered Release of Glutaraldehyde. *Angew. Chem., Int. Ed.* **2017**, *56*, 4724−4728.
(48) Schür, C.; Rist, S.; Baun, A.; Mayer, P.; Hartmann, N. B.; Wagner, M. When Fluorescence Is Not a Particle: The Tissue Translocation of Microplastics in Daphnia Magna Seems an Artifact. *Environ. Toxicol. Chem.* **2019**, *38*, 1495−1503.
(49) Krebs, F. C.; Miller, S. R.; Catalone, B. J.; Welsh, P. A.; Malamud, D.; Howett, M. K.; Wigdahl, B. Sodium Dodecyl Sulfate and C31G as Microbicidal Alternatives to Nonoxynol 9: Comparative Sensitivity of Primary Human Vaginal Keratinocytes. *Antimicrob. Agents Chemother.* **2000**, *44*, 1954−1960.
(50) Radashevsky, V. I.; Yurchenko, O. V.; Alexandrova, Y. N. Fine Structure of the Gametes and Spermiogenesis in Spiophanes Uschakowi (Annelida: Spionidae) from the Sea of Japan, with Comments on Fertilization Biology in Broadcast-Spawning Spionids. *Micron* **2018**, *115*, 32−40.
(51) Della Torre, C.; Bergami, E.; Salvati, A.; Faleri, C.; Cirino, P.; Dawson, K. A.; Corsi, I. Accumulation and Embryotoxicity of Polystyrene Nanoparticles at Early Stage of Development of Sea Urchin Embryos Paracentrotus Lividus. *Environ. Sci. Technol.* **2014**, *48*, 12302−12311.
(52) Al-Sid-Cheikh, M.; Rowland, S. J.; Kaegi, R.; Henry, T. B.; Cormier, M.-A.; Thompson, R. C. Synthesis of 14C-Labelled Polystyrene Nanoplastics for Environmental Studies. *Commun. Mater.* **2020**, *1*, 1−8.
(53) Barnes, H.; Barnes, M. Studies on the Reproduction of Cirripedes. II. Setting of the Lamellae; Action of Protease and Disintegration of the Oviducal Sac. *J. Exp. Mar. Biol. Ecol.* **1977**, *27*, 219−231.
(54) Barnes, H.; Barnes, M. Studies on the Reproduction of Cirripedes. I. Introduction: Copulation, Release of Oocytes, and Formation of the Egg Lamellae. *J. Exp. Mar. Biol. Ecol.* **1977**, *27*, 195−218.
(55) Klepal, W.; Barnes, H.; Barnes, M. Studies on the Reproduction of Cirripedes. VII. The Formation and Fine Structure of the Fertilization Membrane and Egg Case. *J. Exp. Mar. Biol. Ecol.* **1979**, *36*, 53−78.
(56) Wang, C.; Schultzhaus, J. N.; Taitt, C. R.; Leary, D. H.; Shriver-Lake, L. C.; Snellings, D.; Sturiale, S.; North, S. H.; Orihuela, B.; Rittschof, D.; et al. Characterization of Longitudinal Canal Tissue in the Acorn Barnacle Amphibalanus Amphitrite. *PLoS One* **2018**, *13*, No. e0208352.
(57) Jianping, L.; Ruxing, C.; Zhouxing, Q.; Sifeng, W.; Jianwei, Q. Stomach Contents of the Several Barnacles in Zhoushan Waters. *Donghai Mar. Sci.* **1996**, *14*, 28−35.
(58) Hunt, M. J.; Alexander, C. G. Feeding Mechanisms in the Barnacle Tetraclita Squamosa (Bruguière). *J. Exp. Mar. Biol. Ecol.* **1991**, *154*, 1−28.
(59) Crisp, D. J.; Southward, A. J. Different Types of Cirral Activity of Barnacles. *Philos. Trans. R. Soc. London, Ser. B* **1961**, *243*, 271−307.
(60) Walker, G. A. Study of the Oviducal Glands and Ovisacs of Balanus Balanoides (L.) Together with Comparative Observations on the Ovisacs of Balanus Hameri (Ascanius) and the Reproductive Biology of the Two Species. *Philos. Trans. R. Soc. London, Ser. B* **1980**, *291*, 147−162.
(61) Lee, W. S.; Cho, H.-J.; Kim, E.; Huh, Y. H.; Kim, H.-J.; Kim, B.; Kang, T.; Lee, J.-S.; Jeong, J. Bioaccumulation of Polystyrene Nanoplastics and Their Effect on the Toxicity of Au Ions in Zebrafish Embryos. *Nanoscale* **2019**, *11*, 3173−3185.
(62) Duan, Z.; Duan, X.; Zhao, S.; Wang, X.; Wang, J.; Liu, Y.; Peng, Y.; Gong, Z.; Wang, L. Barrier Function of Zebrafish Embryonic

Chorions against Microplastics and Nanoplastics and Its Impact on Embryo Development. *J. Hazard. Mater.* **2020**, *395*, 122621.
(63) Mahadevan, G.; Valiyaveettil, S. Understanding the Interactions of Poly(Methyl Methacrylate) and Poly(Vinyl Chloride) Nanoparticles with BHK-21 Cell Line. *Sci. Rep.* **2021**, *11*, 2089.
(64) Mahadevan, G.; Valiyaveettil, S. Comparison of Genotoxicity and Cytotoxicity of Polyvinyl Chloride and Poly(Methyl Methacrylate) Nanoparticles on Normal Human Lung Cell Lines. *Chem. Res. Toxicol.* **2021**, *34*, 1468−1480.
(65) Cabana, D.; Nicolaidou, A.; Sigala, K.; Reizopoulou, S. Gametogenesis and Spawning Of Spirobranchus Tetraceros (Polychaeta, Serpulidae) in Abu Kir Bay, Egypt. *Mediterr. Mar. Sci.* **2000**, *12*, 121−128.
(66) Belal, A. A. M. Oogenesis and Spawning of Pomatoleious Kraussii (Baired, 1865) (Polychaeta: Serpulidae) in Suez Bay. *Egypt. J. Aquat. Res.* **2012**, *38*, 119−124.
(67) Eckelbarger, K. J. Oogenesis and Oocytes. *Hydrobiologia* **2005**, *535*−*536*, 179−198.
(68) Eckelbarger, K. Vitellogenic Mechanisms and the Allocation of Energy to Offspring in Polychaetes. *Bull. Mar. Sci.* **1986**, *39*, 426−443.
(69) Walczyk, D.; Bombelli, F. B.; Monopoli, M. P.; Lynch, I.; Dawson, K. A. What the Cell "Sees" in Bionanoscience. *J. Am. Chem. Soc.* **2010**, *132*, 5761−5768.
(70) Hayashi, Y.; Miclaus, T.; Murugadoss, S.; Takamiya, M.; Scavenius, C.; Kjaer-Sorensen, K.; Enghild, J. J.; Strähle, U.; Oxvig, C.; Weiss, C.; et al. Female versus Male Biological Identities of Nanoparticles Determine the Interaction with Immune Cells in Fish. *Environ. Sci.: Nano* **2017**, *4*, 895−906.
(71) Gao, J.; Lin, L.; Wei, A.; Sepúlveda, M. S. Protein Corona Analysis of Silver Nanoparticles Exposed to Fish Plasma. *Environ. Sci. Technol. Lett.* **2017**, *4*, 174−179.
(72) Lee, B. K.; Nam, H. J.; Lee, Y. R. Receptor-mediated Transport of Vitellogenin during Oogenesis of a Polychaete, Pseudopotomilla Occelata. *Korean J. Biol. Sci.* **1997**, *1*, 341−344.
(73) Rossi, G.; Barnoud, J.; Monticelli, L. Polystyrene Nanoparticles Perturb Lipid Membranes. *J. Phys. Chem. Lett.* **2014**, *5*, 241−246.
(74) Kettler, K.; Veltman, K.; van de Meent, D.; van Wezel, A.; Hendriks, A. J. Cellular Uptake of Nanoparticles as Determined by Particle Properties, Experimental Conditions, and Cell Type. *Environ. Toxicol. Chem.* **2014**, *33*, 481−492.
(75) Behzadi, S.; Serpooshan, V.; Tao, W.; Hamaly, M. A.; Alkawareek, M. Y.; Dreaden, E. C.; Brown, D.; Alkilany, A. M.; Farokhzad, O. C.; Mahmoudi, M. Cellular Uptake of Nanoparticles: Journey inside the Cell. *Chem. Soc. Rev.* **2017**, *46*, 4218−4244.
(76) Liu, L.; Xu, K.; Zhang, B.; Ye, Y.; Zhang, Q.; Jiang, W. Cellular Internalization and Release of Polystyrene Microplastics and Nanoplastics. *Sci. Total Environ.* **2021**, *779*, 146523.
(77) Oh, N.; Park, J.-H. Surface Chemistry of Gold Nanoparticles Mediates Their Exocytosis in Macrophages. *ACS Nano* **2014**, *8*, 6232−6241.
(78) Yanes, R. E.; Tarn, D.; Hwang, A. A.; Ferris, D. P.; Sherman, S. P.; Thomas, C. R.; Lu, J.; Pyle, A. D.; Zink, J. I.; Tamanoi, F. Involvement of Lysosomal Exocytosis in the Excretion of Mesoporous Silica Nanoparticles and Enhancement of the Drug Delivery Effect by Exocytosis Inhibition. *Small* **2013**, *9*, 697−704.
(79) Kim, C.; Tonga, G. Y.; Yan, B.; Kim, C. S.; Kim, S. T.; Park, M.-H.; Zhu, Z.; Duncan, B.; Creran, B.; Rotello, V. M. Regulating Exocytosis of Nanoparticles via Host-Guest Chemistry. *Org. Biomol. Chem.* **2015**, *13*, 2474−2479.
(80) Bigdeli, A.; Hormozi-Nezhad, M. R.; Parastar, H. Using Nano-QSAR to Determine the Most Responsible Factor(s) in Gold Nanoparticle Exocytosis. *RSC Adv.* **2015**, *5*, 57030−57037.
(81) Mintenig, S. M.; Löder, M. G. J.; Primpke, S.; Gerdts, G. Low Numbers of Microplastics Detected in Drinking Water from Ground Water Sources. *Sci. Total Environ.* **2019**, *648*, 631−635.
(82) Lagarde, F.; Olivier, O.; Zanella, M.; Daniel, P.; Hiard, S.; Caruso, A. Microplastic Interactions with Freshwater Microalgae: Hetero-Aggregation and Changes in Plastic Density Appear Strongly Dependent on Polymer Type. *Environ. Pollut.* **2016**, *215*, 331−339.
(83) Mani, T.; Hauk, A.; Walter, U.; Burkhardt-Holm, P. Microplastics Profile along the Rhine River. *Sci. Rep.* **2015**, *5*, 17988.
(84) Yu, S.-P.; Chan, B. K. K. Intergenerational Microplastics Impact the Intertidal Barnacle Amphibalanus Amphitrite during the Planktonic Larval and Benthic Adult Stages. *Environ. Pollut.* **2020**, *267*, 115560.
(85) Tallec, K.; Paul-Pont, I.; Boulais, M.; Le Goïc, N.; González-Fernández, C.; Le Grand, F.; Bideau, A.; Quéré, C.; Cassone, A.-L.; Lambert, C.; et al. Nanopolystyrene Beads Affect Motility and Reproductive Success of Oyster Spermatozoa (Crassostrea Gigas). *Nanotoxicology* **2020**, *14*, 1039−1057.